

Synthesis, characterization and anticancer activities of transition metal complexes with a nicotinothiohydrazone ligand

SHANSHAN SHEN^{1*}, HONG CHEN^{2*}, TAOFENG ZHU^{2*}, XIUQIN MA², JUN XU³, WENJIAO ZHU², RUHUA CHEN², JING XIE², TIELIANG MA², LEI JIA³, YUAN WANG³ and CHUNYAN PENG¹

¹Department of Gastroenterology, The Affiliated Drum Tower Hospital of Nanjing University Medical School, Nanjing University, Nanjing, Jiangsu 210008; ²The Affiliated Yixing Hospital of Jiangsu University, Yixing, Jiangsu 214200; ³Department of Physics and Chemistry, Henan Polytechnic University, Jiaozuo, Henan 454000, P.R. China

Received September 1, 2015; Accepted January 4, 2017

DOI: 10.3892/ol.2017.5857

Abstract. The reaction of divalent transition metal salts and (E)-N'-(1-(pyridin-2-yl)ethylidene)nicotinothiohydrazide (penh) led to the formation of [Mn(penh)₂] (complex 1), [Co(penh)₂] (complex 2), [Cu(penh)₂] (complex 3) and [Cd(penh)₂] (complex 4) complexes. The four complexes were characterized using elemental analyses, infrared spectra and single-crystal X-ray diffraction analyses. Subsequently, the complexes were used for *in vitro* cell level experiments to determine potential antitumor effects. The results demonstrated that the complexes exhibited a similar structure; however, they were crystallized with distinct space groups. In comparison with the uncomplexed penh ligand, all four complexes were able to markedly decrease the proliferation rate of various types of tumor cell, including the human lung cancer cell line A549, human gastric cancer cell line BGC823 and human esophageal cancer cell line Eca109, in a concentration-dependent manner. Furthermore, the complexes promoted tumor cell apoptosis, as demonstrated in the apoptosis assay, and this was confirmed using electrophoresis.

Introduction

Hydrazide-thiohydrazone derivatives are an important class of biologically active molecules, which have attracted the attention of medicinal chemists due to their wide-ranging pharmacological

properties and their potential application as antitumor, antineoplastic, antiviral and anti-inflammatory agents (1-6).

In particular, thiohydrazone complexes of transition metals are known to provide useful models for the elucidation of the underlying molecular mechanism of enzyme inhibition by hydrazine derivatives (7) and for their potential pharmacological application (8,9). Thiohydrazone derivatives of isoniazid and other hydrazides have been reported to exhibit marked antimicrobial activity (10-14). Furthermore, a number of substituted thiohydrazone derivatives have been synthesized and evaluated for their antitumor activity, with certain promising results having been reported (15-17).

The aim of the present study was to develop potent anticancer agents. (E)-N'-(1-(pyridin-2-yl)ethylidene) nicotinothiohydrazide (penh), and [Mn(penh)₂] (complex 1), [Co(penh)₂] (complex 2), [Cu(penh)₂] (complex 3) and [Cd(penh)₂] (complex 4) metal complexes were synthesized, and their cytotoxicity against human lung cancer (A549), human gastric cancer (BGC823) and human esophageal cancer (Eca109) cell lines was investigated.

Materials and methods

Materials. All starting materials were obtained commercially and used as received. The A549 human lung cancer, BGC823 human gastric cancer and Eca109 human esophageal cancer cell lines were obtained from the Cell Culture Center of the Basic Institute of Medical Sciences (Peking Union Medical College, Beijing, China). Cell culture reagents were purchased from Gibco (Thermo Fisher Scientific, Inc., Waltham, MA, USA). An Annexin V/propidium iodide (PI) double staining kit was purchased from BD Biosciences (Franklin Lakes, NJ, USA). MTT and dimethyl sulfoxide (DMSO) were purchased from Sigma-Aldrich (Merck KGaA, Darmstadt, Germany). Polyvinylidene fluoride (PVDF) membranes and non-fat dried milk were obtained from EMD Millipore (Billerica, MA, USA). Polyclonal antibodies against p53 (cat. no. 3036), apoptosis regulator Bax (Bax) (cat. no. 3032) and apoptosis regulator Bcl-2 (Bcl-2) (cat. no. 3195) were obtained from BioVision, Inc. (Milpitas, CA, USA). Anti-GAPDH (cat. no. E7EUT5) polyclonal antibody was purchased from Abmart, Inc. (Shanghai, China). The alkaline phosphatase (AP)-conjugated anti-mouse IgG (cat. no. A0258) and AP-conjugated anti-rabbit IgG (cat. no. A0239) secondary

Correspondence to: Dr Chunyan Peng, Department of Gastroenterology, The Affiliated Drum Tower Hospital of Nanjing University Medical School, Nanjing University, 321 Zhongshan Road, Nanjing, Jiangsu 210008, P.R. China
E-mail: springpcy@aliyun.com

Ms. Xiuqin Ma, The Affiliated Yixing Hospital of Jiangsu University, 75 Tongzhenguan Road, Yixing, Jiangsu 214200, P.R. China
E-mail: staff799@yxph.com

*Contributed equally

Key words: transition metal complexes, nicotinothiohydrazone ligand, anticancer

antibodies were obtained from the Beyotime Institute of Biotechnology (Haimen, China).

Elemental analyses (concentration of each complex, 1.25×10^{-5} mol/l) were performed in the Microanalytical Laboratory of the Department of Chemistry of Lanzhou University (Lanzhou, China). ^1H nuclear magnetic resonance (NMR) spectra were recorded using an ACF300 Fourier-transform NMR instrument (Bruker Corporation, Billerica, MA, USA) using tetramethylsilane as an internal reference in $[\text{D}_6]\text{DMSO}$ for the ligand. The infrared spectra (KBr pellet) were recorded using an FTS165 Fourier-transform infrared spectrophotometer (Bio-Rad Laboratories, Inc., Hercules, CA, USA) between 4,000 and 400 cm^{-1} (18). Molecular structures were drawn using ChemDraw[®] Pro plugin (version 8.0; Cambridge Soft; PerkinElmer Inc., Waltham, MA, USA).

Compound synthesis

Synthesis of the penh ligand. An ethanol solution (30 ml) containing salicylaldehyde (1.21 g, 10 mmol) was added dropwise to another ethanol solution (30 ml) containing the nicotinohydrazide (1.37 g, 10 mmol). Following reflux for 6 h, the mixture was cooled to room temperature, and the white precipitate solid was collected by suction filtration and washed with ice-cold ethanol. The penh ligand was collected following recrystallization using anhydrous methanol and was dried under a vacuum. The yield was 93.1%. ^1H -NMR (C^2HCl_3 , ppm) 7.41–9.15 (8H, m, Ar-H), 2.56 (3H, s, CH_3). Infrared (IR) (KBr, cm^{-1}): $\nu(\text{OH})$ 3486, $\nu(\text{N-N})$ 3,190, $\nu(\text{C=O})$ 1,667, $\nu(\text{C=N})$ 1,580. Elemental analysis for penh ($\text{C}_{52}\text{H}_{50}\text{N}_{19}\text{O}_{14}$): C, 53.61; H, 4.33; N, 22.84 (calculated); C, 53.56; H, 4.51; N, 22.89 (found).

Synthesis of the complexes. Complex 1 was prepared as follows: The penh ligand (1 mmol, 0.241 g) containing 3 drops of triethylamine was dissolved in 30 ml anhydrous methanol, MnCl_2 (0.5 mmol, 0.063 g) in anhydrous methanol (10 ml) was then added dropwise with stirring. After 1 week, single crystals of 1 suitable for X-ray diffraction were obtained from the reaction solution. Crystals were separated from the solution by suction filtration, purified by washing several times with ethanol. The yield was 58.3%. Elemental analysis for 1 ($\text{C}_{26}\text{H}_{22}\text{MnN}_8\text{O}_2$): C, 58.54; H, 4.16; N, 21.01 (calculated); C, 58.59; H, 4.22; N, 21.20 (found). IR (KBr, cm^{-1}): $\nu(\text{OH})$ 3,461, $\nu(\text{C=N})$ 1,517.

The preparation of complex 2 was similar to that of complex 1, using CoCl_2 instead of MnCl_2 . The yield was 68.5%. Elemental analysis for complex 2 ($\text{C}_{26}\text{H}_{22}\text{CoN}_8\text{O}_2$): C, 58.10; H, 4.13; N, 20.85 (calculated); C, 58.25; H, 4.25; N, 21.04 (found). IR (KBr, cm^{-1}): $\nu(\text{OH})$ 3,472, $\nu(\text{C=N})$ 1,516.

The preparation of complex 3 was similar to that of complex 1, using CuCl_2 instead of MnCl_2 . The yield was 66.1%. Elemental analysis for complex 3 ($\text{C}_{26}\text{H}_{22}\text{CuN}_8\text{O}_2$): C, 57.61; H, 4.09; N, 20.67 (calculated); C, 57.72; H, 4.18; N, 20.77 (found). IR (KBr, cm^{-1}): $\nu(\text{OH})$ 3,480, $\nu(\text{C=N})$ 1,515.

The preparation of complex 4 was similar to that of complex 1, using CdCl_2 instead of MnCl_2 . The yield was 53.5%. Elemental analysis for complex 4 ($\text{C}_{26}\text{H}_{22}\text{CdN}_8\text{O}_2$): C, 52.85; H, 3.75; N, 18.96 (calculated); C, 52.99; H, 3.86; N, 19.16 (found). IR (KBr, cm^{-1}): $\nu(\text{OH})$ 3,481, $\nu(\text{C=N})$ 1,516.

X-ray crystallography. The X-ray diffraction measurements for two complexes were performed on a SMART APEX II

charge-coupled device diffractometer (Bruker Corporation) equipped with graphite monochromatized Mo-K radiation ($\lambda=0.071073\text{ nm}$) using ϕ - ω scan mode. Semi-empirical absorption correction was applied to the intensity data using the SADABS program (version 2.03; Bruker AXS, Inc., Billerica, MA, USA) (19). The structures were solved and refined by full-matrix least-squares on F^2 using the SHELXTL-97 program (Bruker AXS, Inc.) (20). All non-H atoms were refined anisotropically. All H atoms were positioned geometrically and refined using a riding model (18). Details of the crystal parameters, data collection and refinement for complexes 1–4 are summarized in Table I.

Cytotoxic activity of the complexes. To evaluate whether or not complexes 1–4 exhibit a tumor cell killing ability, the effect of DMSO-soluble complexes 1–4 on A549 (lung cancer), BGC823 (gastric cancer) and Eca109 (esophageal cancer) human solid tumor cell lines was investigated. All three cell lines were cultured in RPMI-1640 medium supplemented with 10% fetal bovine serum, 100 units/ml penicillin and $100\text{ }\mu\text{g/ml}$ streptomycin at 37°C in a humidified atmosphere containing 5% CO_2 . The effect of treatment with complexes 1–4 on the survival of the three human tumor cell lines was assessed using an MTT assay in distilled water. Cells were seeded in 96-well plates at 1×10^4 cells/well. Following overnight growth, the cells were cultured for 72 h in the presence of 3, 6, 9, 12, 15, 18 and $21\text{ }\mu\text{mol/l}$ complexes 1–4, with cells cultured with the corresponding uncomplexed penh ligand serving as the control group. After 72 h incubation, $20\text{ }\mu\text{l}$ MTT was added into each well and cells were incubated at 37°C for 4 h. Culture medium was removed and $150\text{ }\mu\text{l}$ DMSO was added. The plates were agitated, prior to determination of the optical density at 570 nm using an ELISA plate reader. Images of cells were captured using an upright metallurgical microscope (BX61; magnification, $\times 20$; Olympus Corporation, Tokyo, Japan). At least three parallel experiments were performed. As complex 3 exhibited increased cytotoxic activity compared with the other complexes, particularly for the Eca109 cell line, Eca109 cells and complex 3 were selected for subsequent cell apoptosis assay and western blot analysis.

Quantification of apoptosis using Annexin V and PI double staining. Apoptotic rates were determined using flow cytometry using an Annexin V/PI apoptosis kit. Eca109 cancer cells were seeded at a density of 1×10^6 cells/well in 6-well plates, cultured overnight, and treated with 3, 6 and $9\text{ }\mu\text{mol/l}$ complex 3 for 48 h at 37°C . After 48 h, the cells were collected by centrifugation at $200 \times g$ for 5 min at 4°C and washed twice with ice-cold PBS. Staining was carried out according to the manufacturer's protocol, and the cells were analyzed using a BD Acurri[™] C6 flow cytometer (BD Biosciences) and analyzed using CellQuest software (version 6.0; BD Biosciences). Each experiment was carried out at least three times independently.

Western blot analysis. Eca109 cancer cells were seeded in 6-well plates overnight. Cells were treated with $4\text{ }\mu\text{mol/l}$ complex 3 for 48 h at 37°C . Total proteins were collected and protein concentration was determined using a bicinchoninic acid protein assay. Proteins ($20\text{ }\mu\text{g}$) were separated by SDS-PAGE

Table I. Crystal data and structure refinement for the complexes.

Characteristic	[Mn(penh) ₂]	[Co(penh) ₂]	[Cu(penh) ₂]	[Cd(penh) ₂]
Empirical formula	C ₂₆ H ₂₂ N ₈ O ₂ Mn	C ₂₆ H ₂₂ N ₈ O ₂ Co	C ₂₆ H ₂₂ N ₈ O ₂ Cu	C ₂₆ H ₂₂ N ₈ O ₂ Cd
Formula mass	533.46	537.45	542.06	590.92
Temperature, K (±SD)	296 (2)	296 (2)	296 (2)	296 (2)
Wavelength, nm	0.071073	0.071073	0.071073	0.071073
Crystal system	Orthorhombic	Orthorhombic	Orthorhombic	Monoclinic
Space group	Pbca	Aba2	Pbca	Cc
Z	8	8	8	4
a, Å	11.9900 (10)	12.114 (2)	11.965 (3)	20.761 (5)
b, Å	10.3280 (8)	19.088 (4)	10.306 (3)	14.905 (4)
c, Å	39.095 (3)	10.3482 (19)	39.234 (11)	8.1989 (19)
β, °	-	-	-	105.064 (3)
V, Å ³	4,841.2 (7)	2,392.8 (8)	4,838 (2)	2,449.9 (10)
D _{calc} , g·cm ⁻³	1.464	1.492	1.488	1.602
μ, mm ⁻¹	0.587	0.760	0.945	0.933
F(000)	2,200	1,108	2,232	1,192
Independent reflections (R _{int})	4,261 (0.0815)	1,535 (0.0528)	4,261 (0.0755)	3,969 (0.0129)
Final GooF	1.048	1.026	1.100	1.055
R ₁ , wR ₂ [I>2σ(I)]	R ₁ = 0.0641 wR ₂ = 0.1806	R ₁ = 0.0439 wR ₂ = 0.1069	R ₁ = 0.0680 wR ₂ = 0.1734	R ₁ = 0.0254 wR ₂ = 0.0692
R ₁ , wR ₂ (all data)	R ₁ = 0.1145 wR ₂ = 0.2117	R ₁ = 0.0643 wR ₂ = 0.1203	R ₁ = 0.1043 wR ₂ = 0.1966	R ₁ = 0.0269 wR ₂ = 0.0707

The numbers in parentheses indicate the standard deviation of the bond distances to the third decimal place. penh, (E)-N'-(1-(pyridin-2-yl)ethylidene)nicotinohydrazide; Z, cell formula units; a, b and c, cell lengths; β, cell angle; V, cell volume; D_{calc}, crystal density; μ, absorption coefficient; F(000), number of electrons in a single crystal; R_{int}, independent reflections; R₁, value of all diffraction points; wR₂, value of observable diffraction points; GooF, goodness of fit.

(12% gel), transferred onto PVDF membranes by electroblotting and probed with antibodies against p53 (1:1,000), Bax (1:1,000), Bcl-2 (1:1,000) and GAPDH (1:2,000) diluted in 5% BSA (cat. no. 10711454001; Roche Applied Science, Penzberg, Germany) and blocked using 5% dried skimmed milk overnight at 4°C. The membranes were incubated with secondary antibody against IgG labeled with AP and detected using a Lumi-Phos™ WB enhanced chemiluminescence kit (Thermo Fisher Scientific, Inc.) at room temperature. Membranes were scanned using an HP ScanJet G4010 flatbed scanner (HP, Inc., Palo Alto, CA, USA).

Statistical analysis. Statistical analysis was performed using SAS software (version 6.12; SAS Institute, Inc., Cary, NC, USA). Measurement data are presented as the mean ± standard deviation. To compare the differences between the groups, statistical significance was determined using a one-way analysis of variance followed by Dunnett's test comparisons. P<0.05 was considered to indicate a statistically significant difference.

Results and Discussion

Crystal structures of complexes 1-4. Structures of the four complexes are presented in Fig. 1. The complexes exhibited similar structures; however, they were crystallized in distinct space groups (Table I). In each complex, the metal center with a

distorted octahedron geometry was identified to be surrounded by two molecules of monoanionic ligand, which coordinates to the metal ion with an N₂O donor set, namely deprotonated carbonylate-O, azomethine-N and pyridyl-N atoms. The N₂O donor sites of the tridentate ligand formed four five-membered CN₂OM (where M represents the transition metal) and C₂N₂M chelate rings around the metal ion. The carbonyl bond distances of Mn(II), Ni(II), Cu(II) and Zn(II) complexes were between 1.256 (±0.006) and 1.277 (±0.006) Å, confirming the formation of the M-O bond through an enolized C-O group (21). In addition, the distances of the enolized C-O and imine C-N bands in the complexes were intermediate between single and double bond, suggesting an extended conjugation in anionic ligand following complexation. The M-O and M-N bond lengths (Table II) were in the normal range reported for Mn(II), Co(II), Cu(II) and Cd(II) octahedral complexes (22). As predicted, there were no classical hydrogen bonds in any of the complexes.

IR spectra of the complexes. The IR spectra of the four complexes were similar. The ν(C=O) of the uncomplexed penh ligand were at 1,667 cm⁻¹; for complexes, this peak disappeared, indicating that the amide group was involved in coordination to the metal ion through the enol form. The band at 1,580 cm⁻¹ for the uncomplexed penh ligand was assigned to the ν(C=N) stretch, which shifted to near 1,518 cm⁻¹ for the

Table II. Selected bond lengths and angles in the four complexes.

A, [Mn(penh) ₂] bonds	
Bond	Length, Å
Mn1-N6	2.061 (5)
Mn1-N2	2.065 (5)
Mn1-O2	2.124 (4)
Mn1-O1	2.174 (4)
Mn1-N1	2.193 (5)
Mn1-N5	2.198 (5)
B, [Mn(penh) ₂] angles	
Angle	Size, °
N6-Mn1-N2	172.67 (18)
N6-Mn1-O2	75.45 (17)
N2-Mn1-O2	107.99 (16)
N6-Mn1-O1	99.32 (16)
N2-Mn1-O1	73.88 (16)
O2-Mn1-O1	99.41 (18)
N6-Mn1-N1	111.24 (18)
N2-Mn1-N1	75.32 (18)
O2-Mn1-N1	93.49 (17)
O1-Mn1-N1	148.98 (16)
N6-Mn1-N5	74.57 (18)
N2-Mn1-N5	102.69 (17)
O2-Mn1-N5	149.03 (17)
O1-Mn1-N5	92.90 (16)
N1-Mn1-N5	90.21 (17)
C, [Co(penh) ₂] bonds	
Bond	Length, Å
Co1-N2	2.032 (4)
Co1-O1	2.081 (4)
Co1-N1	2.134 (5)
D, [Co(penh) ₂] angles	
Angle	Size, °
N2-Co1-N2 ⁱ	174.71 (4)
N2-Co1-O1 ⁱ	101.14 (18)
N2-Co1-O1	75.57 (18)
O1-Co1-O1 ⁱ	104.82 (3)
N2-Co1-N1	75.40 (2)
O1-Co1-N1	148.85 (15)
O1-Co1-N1 ⁱ	91.61 (18)
N2-Co1-N1 ⁱ	108.65 (2)
N1-Co1-N1 ⁱ	87.25 (3)
O1-Co1-N1 ⁱ	91.61 (18)
N2-Co1-N1 ⁱ	108.67 (2)
N1-Co1-N1 ⁱ	87.26 (3)

Table II. Continued.

E, [Cu(penh) ₂] bonds	
Bond	Length, Å
Cu1-N6	2.002 (5)
Cu1-N2	1.948 (5)
Cu1-O2	2.268 (4)
Cu1-O1	2.073 (4)
Cu1-N1	2.079 (5)
Cu1-N5	2.280 (5)
F, [Cu(penh) ₂] angles	
Angle	Size, °
N6-Cu1-N2	172.96 (2)
N6-Cu1-O2	74.07 (17)
N2-Cu1-O2	98.86 (17)
N6-Cu1-O1	103.07 (17)
N2-Cu1-O1	78.03 (18)
O2-Cu1-O1	97.86 (18)
N6-Cu1-N1	100.84 (18)
N2-Cu1-N1	78.62 (19)
O2-Cu1-N1	91.63 (17)
O1-Cu1-N1	155.88 (17)
N6-Cu1-N5	76.37 (19)
N2-Cu1-N5	110.65 (19)
O2-Cu1-N5	150.22 (16)
O1-Cu1-N5	92.22 (18)
N1-Cu1-N5	90.37 (19)
G, [Cd(penh) ₂] bonds	
Bond	Length, Å
Cd1-N6	2.266 (3)
Cd1-N2	2.265 (3)
Cd1-O2	2.291 (3)
Cd1-O1	2.258 (3)
Cd1-N1	2.362 (3)
Cd1-N5	2.356 (3)
H, [Cd(penh) ₂] angles	
Angle	Size, °
N6-Cd1-N2	169.29 (10)
N6-Cd1-O2	69.15 (9)
N2-Cd1-O2	100.32 (9)
N6-Cd1-O1	113.59 (10)
N2-Cd1-O1	69.61 (10)
O2-Cd1-O1	102.07 (11)
N6-Cd1-N1	106.78 (10)
N2-Cd1-N1	69.83 (9)
O2-Cd1-N1	87.61 (11)
O1-Cd1-N1	139.36 (10)

Table II. Continued.

H, [Cd(penh) ₂] angles	
Angle	Size, °
N6-Cd1-N5	69.98 (10)
N2-Cd1-N5	120.21 (10)
O2-Cd1-N5	138.62 (10)
O1-Cd1-N5	99.71 (9)
N1-Cd1-N5	98.14 (10)

Symmetry code: (i) -x, 2-y, z. penh, (E)-N'-(1-(pyridin-2-yl)ethylidene)nicotinohydrazide.

complexes, indicating that the N atom of C=N was involved in coordination to the metal ion. The vibrations $\nu(\text{N-H})$ disappeared in the spectra of the four complexes, indicating that the ligand was deprotonated. The novel bands near 560 cm^{-1} for the complexes were assigned to $\nu(\text{M-O})$, and the weaker peaks near 470 cm^{-1} were assigned to $\nu(\text{M-N})$, respectively (23,24), consistent with the results of X-ray diffraction analysis.

Antitumor activity of the four complexes. The four complexes were air-stable for extended periods and soluble in methanol, dimethylformamide and DMSO, slightly soluble in water, and insoluble in benzene and diethyl ether. The stability of the complexes in DMSO were determined by observing the ultraviolet (UV)-visible spectra at distinct time intervals for any potential alteration. The Cu(II) complexes investigated were prepared in DMSO and were freshly diluted in phosphate buffer (pH 7.4) for experiments. The UV-visible spectra were subsequently analyzed at various intervals. The results indicate that the UV-visible spectra remained unaltered in solution for the entire course of the experiment (72 h) and that the complexes are stable in solution.

It has been reported that arylhydrazone and its metal complexes exhibit markedly effective antitumor activities, possibly due to their NO bidentate systems (24). *In vitro* cytotoxicity assays were carried out in the human A549 (human lung cancer), BGC823 (human gastric cancer) and Eca109 (human esophageal cancer) solid tumor cell lines. Following co-culture with each complex, cell proliferation was markedly inhibited. As presented in Fig. 2, alterations in tumor cell morphology, including cell shrinkage and cell detachment, were observed. Cell survival and proliferation were determined using the MTT assay. The half-maximal inhibitory concentration (IC_{50})

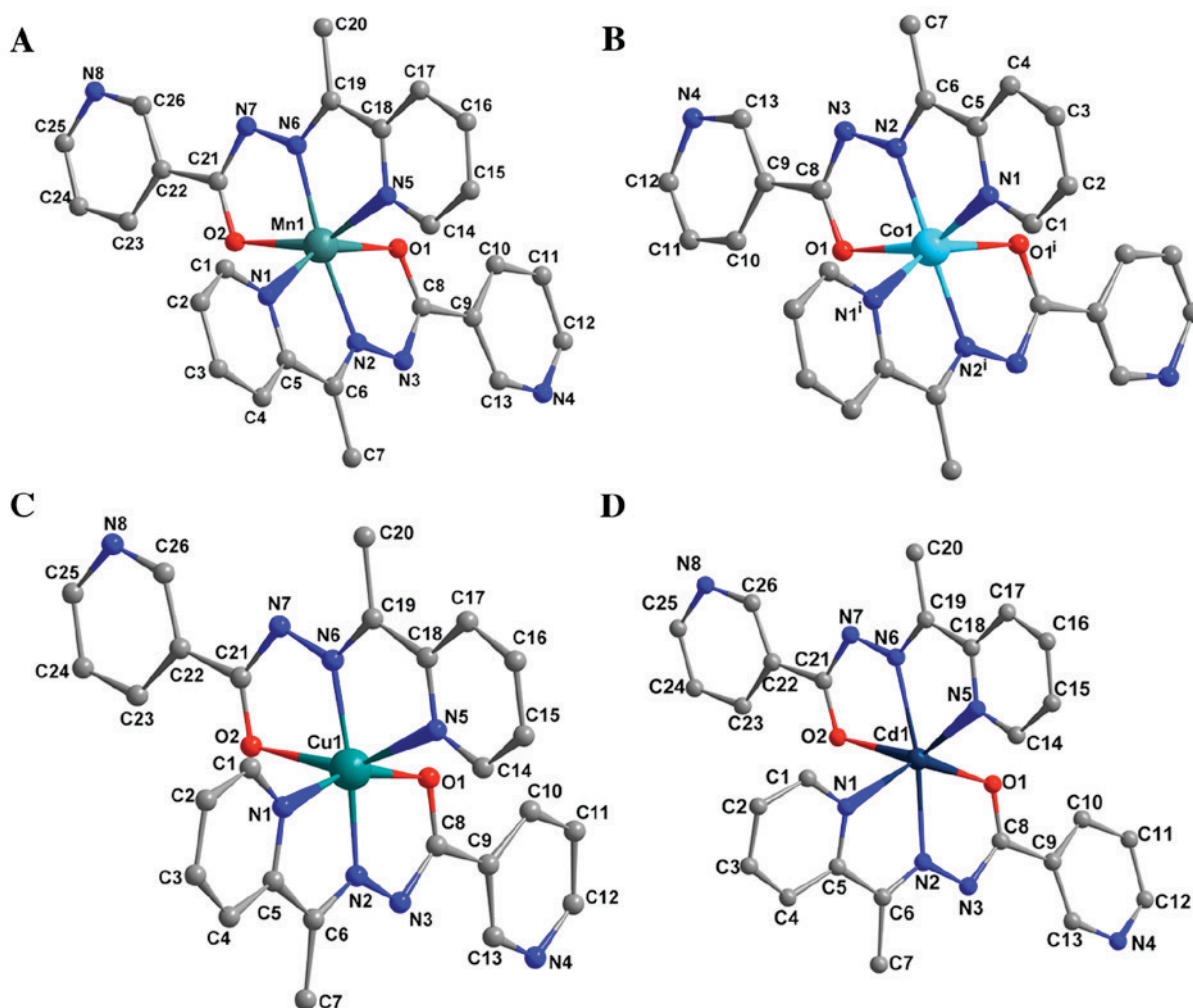


Figure 1. Molecular structures of (A) $[\text{Mn}(\text{penh})_2]$, (B) $[\text{Co}(\text{penh})_2]$, (C) $[\text{Cu}(\text{penh})_2]$ and (D) $[\text{Cd}(\text{penh})_2]$ drawn using ChemDraw[®] Pro plugin (version 8.0; Cambridge Soft; PerkinElmer, Inc.). H atoms are omitted for clarity; symmetry code: (i) -x, 2-y, z. penh, (E)-N'-(1-(pyridin-2-yl)ethylidene)nicotinohydrazide.

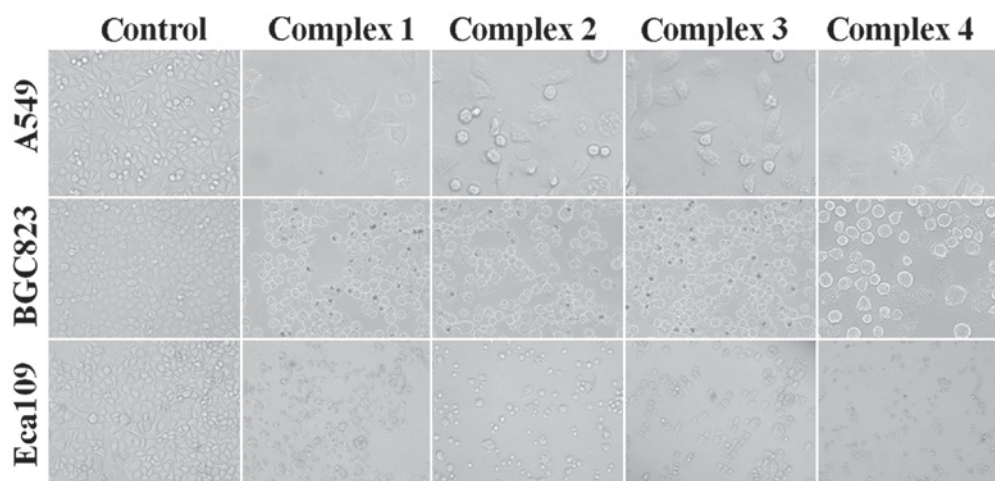


Figure 2. Phase-contrast micrographs of cell lines treated with control [uncomplexed ligand (E)-N'-(1-(pyridin-2-yl)ethylidene)nicotinohydrazide] and complexes 1-4 (magnification, x20).

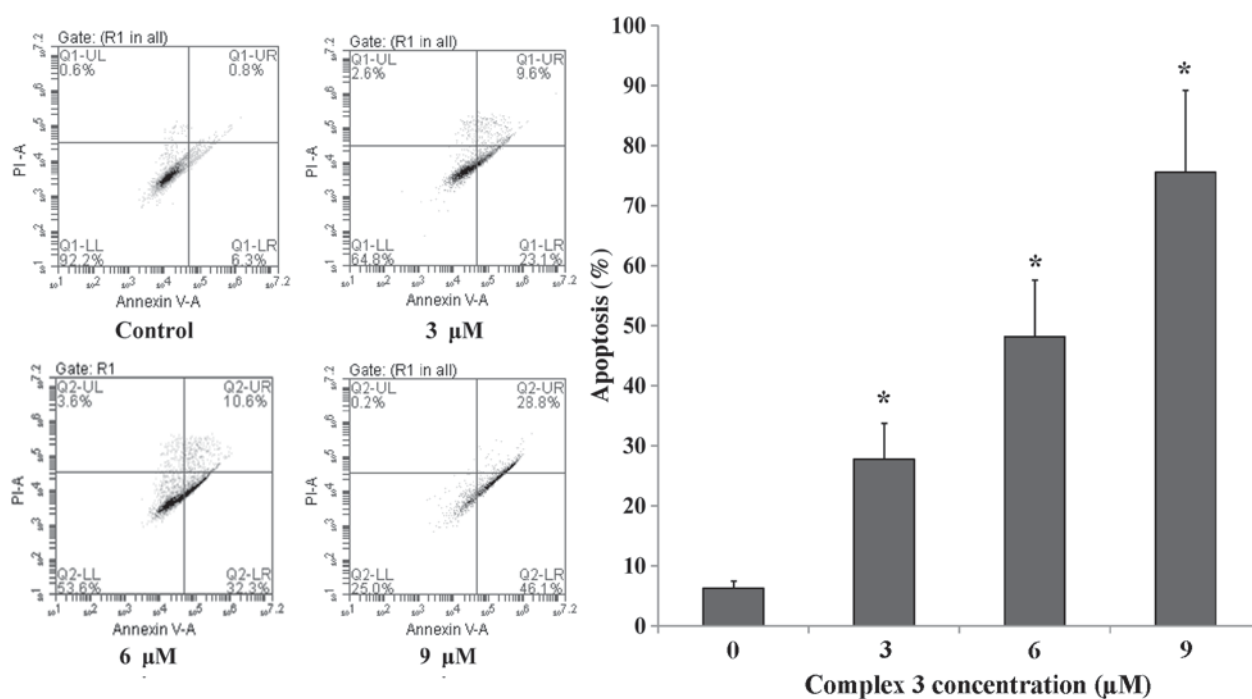


Figure 3. Detection of apoptosis in Eca109 cells following treatment with complex 3 using Annexin V/PI staining. Left panel, representative flow cytometry results; right panel, quantification of flow cytometric results. PI, propidium iodide; A, area; Q, quadrant; UL, upper left; UR, upper right; LL, lower left; LR, lower right. * $P < 0.05$.

Table III. Half-maximal inhibitory concentration ($\mu\text{mol/l}$) values for the uncomplexed (E)-N'-(1-(pyridin-2-yl)ethylidene)nicotinohydrazide ligand and complexes 1-4 in human lung cancer (A549), human gastric cancer (BGC823) and human esophageal cancer (Eca109) cell lines.

Compound	A549	BGC823	Eca109
Ligand	156.5	196.8	165.1
Complex 1	12.2	18.3	9.6
Complex 2	8.1	11.8	10.3
Complex 3	7.3	9.7	6.5
Complex 4	13.5	15.6	11.9

values are presented in Table III. Complexes 1-4 exhibited significantly decreased IC_{50} values in comparison with that of uncomplexed penh ligand for all three cell lines used ($P < 0.05$). These results demonstrate that the complexes are able to inhibit tumor cell proliferation, and the effect was increased compared with the uncomplexed penh ligand, which suggested that the coordinated transition metal in complexes 1-4 serves a major role in mediating potency of the complexes. The results of the MTT assay demonstrated that complex 1 and 4 exhibited similar IC_{50} values for the three human tumor cell lines, whereas complex 3 exhibited increased cytotoxic activity compared with the other complexes, particularly for the Eca109 cell line. Therefore, Eca109 cells and complex 3

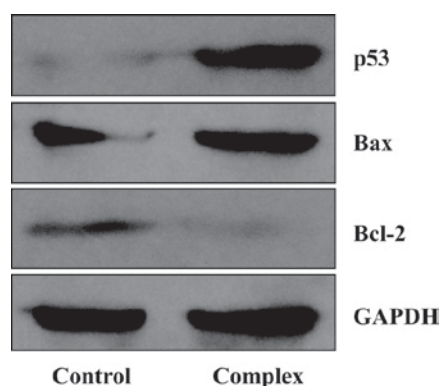


Figure 4. Western blot analysis of expression levels of the p53, Bax and Bcl-2 proteins in Eca109 cells following treatment with complex 3. Bax, apoptosis regulator Bax; Bcl-2, apoptosis regulator Bcl-2.

were selected for subsequent cell apoptosis assay and western blot analysis.

Complex 3 induces cell apoptosis. To determine whether the decrease in human tumor cell growth was attributable to the induction of apoptosis of cancer cells, Annexin V/PI staining and flow cytometric measurement were used to quantify the level of apoptosis. Following incubation with 3, 6 and 9 $\mu\text{mol/l}$ complex 3 for 48 h, the number of apoptotic cells of Eca109 was determined. As presented in Fig. 3, the number of apoptotic Eca109 cells was increased significantly compared with the untreated control in a dose-dependent manner ($P < 0.05$).

Alterations in apoptotic protein expression in tumor cells. To investigate the underlying molecular mechanism of how complexes 1-4 induce apoptosis in cancer cells, levels of proteins that serve important roles in apoptosis, including p53, Bax and Bcl-2, were determined. According to previous studies (25-27), p53 and Bcl-2 family proteins are key regulators of the apoptotic signaling pathway. Following stimulation of internal and external factors, the expression level of protein p53 and Bax is increased in the cells, promoting apoptosis. By contrast, Bcl-2 inhibits apoptosis by preventing the release of cytochrome *c* from mitochondria into the cytoplasm. In the present study, following incubation with 4 $\mu\text{mol/l}$ complex 3 for 48 h, the levels of p53 and Bax protein were increased, whereas the expression of Bcl-2 protein was markedly decreased (Fig. 4).

In the present study, four isostructural divalent transition metal complexes with the nicotinohydrazone (penh) ligand were isolated and characterized using elemental analysis, infrared spectroscopy and single-crystal X-ray diffraction. The results of the present study indicate that the complexes demonstrate marked cytotoxic activity against three cancer cell lines (A549 human lung cancer, BGC823 human gastric cancer and Eca109 human esophageal cancer), and the IC_{50} values for the metal complexes were decreased compared with that of the nicotinohydrazone (penh) ligand. Furthermore, the complexes were also demonstrated to induce apoptosis of the cancer cells, as demonstrated using the Annexin V/PI staining and western blot analysis. Therefore, the results of the present study suggest that complexes 1-4 have potential practical application, acting as novel therapeutic reagents in the treatment of cancer.

Acknowledgements

The present study was supported in part by the National Natural Science Foundation of China (grant nos. 21404033, 21001040 and 81201908), the Fund of Clinical Science and Technology of Wuxi (grant no. Q201512), the Foundation of the Social Development Project of Jiangsu (grant no. BE2015621), the Natural Science Foundation of Jiangsu (grant no. BK20141122), and the Medical Science and Technology Development Projects of Nanjing City (grant no. YKK 14061).

References

- Howard RA, Sherwood E, Erck A, Kimball AP and Bear JL: Hydrophobicity of several rhodium (II) carboxylates correlated with their biologic activity. *J Med Chem* 20: 943-946, 1977.
- Melnyk P, Leroux V, Sergheraert C and Grellier P: Design, synthesis and in vitro antimalarial activity of an acylhydrazone library. *Bioorg Med Chem Lett* 16: 31-35, 2006.
- Wardakhan WW, El-Sayed NN and Mohareb RM: Synthesis and anti-tumor evaluation of novel hydrazide and hydrazide-hydrazone derivatives. *Acta Pharm* 63: 45-57, 2013.
- Aranha PE, dos Santos MP, Romera S and Dockal ER: Synthesis, characterization, and spectroscopic studies of tetradentate Schiff base chromium (III) complexes. *Polyhedron* 26: 1373-1382, 2007.
- Bernhardt PV, Chin P, Sharpe PC, Wang JY and Richardson DR: Novel diaroilylhydrazine ligands as iron chelators: Coordination chemistry and biological activity. *J Biol Inorg Chem* 10: 761-777, 2005.
- Suzen S, Tekiner-Gulbas B, Shirinzadeh H, Uslu D, Gurer-Orhan H, Gumustas M and Ozkan SA: Antioxidant activity of indole-based melatonin analogues in erythrocytes and their voltammetric characterization. *J Enzyme Inhib Med Chem* 28: 1143-1155, 2013.
- Shaabani B, Khandar AA, Mobaiyen H, Ramazani N, Balula SS and Cunha-Silva L: Novel pseudohalide-bridged Cu(II) complexes with a hydrazone ligand: Evaluation of antimicrobial activity. *Polyhedron* 80: 166-172, 2014.
- Drover MW, Tandon SS, Anwar MU, Shuvaev KV, Dawe LN, Collins JL and Thompson LK: Polynuclear complexes of a series of hydrazone and hydrazone-oxime ligands-M2 (Fe), M4 (Mn, Ni, Cu) and Mn (Cu) examples. *Polyhedron* 68: 94-102, 2014.
- Banerjee S, Sen S, Basak S, Mitra S, Hughes DL and Desplanches C: Two new pseudohalide-bridged Cu (II) complexes with a hydrazone ligand: Syntheses, crystal structures and magnetic studies. *Inorganica Chimica Acta* 361: 2707-2714, 2008.
- Rollas S and Küçükgüzel SG: Biological activities of hydrazone derivatives. *Molecules* 12: 1910-1939, 2007.
- Narang R, Narasimhan B and Sharma S: A review on biological activities and chemical synthesis of hydrazide derivatives. *Curr Med Chem* 19: 569-612, 2012.
- Judge V, Narasimhan B and Ahuja M: Isoniazid: The magic molecule. *Med Chem Res* 21: 3940-3957, 2012.
- Vicini P, Zani F, Cozzini P and Doytchinova I: Hydrazones of 1,2-benzisothiazole hydrazides: Synthesis, antimicrobial activity and QSAR investigations. *Eur J Med Chem* 37: 553-564, 2002.
- Kumar P, Narasimhan B, Sharma D, Judge V and Narang R: Hansch analysis of substituted benzoic acid benzylidene/furan-2-yl-methylene hydrazides as antimicrobial agents. *Eur J Med Chem* 44: 1853-1863, 2009.
- Altıntop MD, Özdemir A, Turan-Zitouni G, Ilgin S, Atlı Ö, Demirci F and Kaplancıklı ZA: Synthesis and in vitro evaluation of new nitro-substituted thiazolyl hydrazone derivatives as anticandidal and anticancer agents. *Molecules* 19: 14809-14820, 2014.
- Zhang B, Zhao Y, Zhai X, Wang L, Yang J, Tan Z and Gong P: Design, synthesis and anticancer activities of diaryl urea derivatives bearing N-acylhydrazone moiety. *Chem Pharm Bull (Tokyo)* 60: 1046-1054, 2012.
- Xia Y, Fan CD, Zhao BX, Zhao J, Shin DS and Miao JY: Synthesis and structure-activity relationships of novel 1-arylmethyl-3-aryl-1H-pyrazole-5-carbohydrazone hydrazone derivatives as potential agents against A549 lung cancer cells. *Eur J Med Chem* 43: 2347-2353, 2008.

18. Jia L, Xu J, Zhao X, Shen S, Zhou T, Xu Z, Zhu T, Chen R, Ma T, Xie J, *et al*: Synthesis, characterization, and antitumor activity of three ternary dinuclear copper (II) complexes with a reduced Schiff base ligand and diimine coligands in vitro and in vivo. *J Inorg Biochem* 159: 107-119, 2016.
19. Sheldrick G: SADABS, Program for Empirical Absorption Correction of Area Detector Data. University of Göttingen, Göttingen, Germany, 1996.
20. Sheldrick G: SHELX-97, Program for the Solution and Refinement of Crystal Structures. University of Göttingen, Göttingen, Germany, 1997.
21. Singh P, Singh DP and Singh VP: Synthesis, spectral and single crystal X-ray diffraction studies on Mn(II), Ni(II), Cu(II) and Zn(II) complexes with 2-hydroxy-benzoic acid (phenyl-pyridin-2-yl-methylene)-hydrazide. *Polyhedron* 81: 56-65, 2014.
22. Krishnamoorthy P, Sathyadevi P, Cowley AH, Butorac RR and Dharmaraj N: Evaluation of DNA binding, DNA cleavage, protein binding and in vitro cytotoxic activities of bivalent transition metal hydrazone complexes. *Eur J Med Chem* 46: 3376-3387, 2011.
23. Lewis FD and Barancyk SV: Lewis acid catalysis of photochemical reactions. 8. Photodimerization and cross-cycloaddition of coumarin. *J Am Chem Soc* 111: 8653-8661, 1989.
24. Hao ZY, Liu QW, Xu J, Jia L and Li SB: Synthesis, characterization, antioxidant activities, and DNA-binding studies of (E)-N'-[1-(pyridin-2-yl)ethylidene] isonicotinohydrazide and its Pr (III) and Nd (III) complexes. *Chem Pharm Bull (Tokyo)* 58: 1306-1312, 2010.
25. Pflaum J, Schlosser S and Müller M: p53 family and cellular stress responses in cancer. *Front Oncol* 4: 285, 2014.
26. Mihara M, Erster S, Zaika A, Petrenko O, Chittenden T, Pancoska P and Moll UM: p53 has a direct apoptogenic role at the mitochondria. *Mol Cell* 11: 577-590, 2003.
27. Chipuk JE, Kuwana T, Bouchier-Hayes L, Droin NM, Newmeyer DD, Schuler M and Green DR: Direct activation of Bax by p53 mediates mitochondrial membrane permeabilization and apoptosis. *Science* 303: 1010-1014, 2004.